A Preclinical Model of Minimal Residual Cancer in the Muscle Highlights Challenges Associated with Adenovirus-mediated *p53* Gene Transfer

Roth Oakley, Elaine Phillips, Richard Hooper, Deborah Wilson, and Max Partridge[1]

Maxillofacial Surgery/Oncology, King's College Hospital, London SE5 8RX, United Kingdom [R. O., E. P., M. P.]; Department of Public Health Sciences, GKT School of Medicine, London SE1 3QD, United Kingdom [R. H.]; and Introgen Therapeutics Inc., Houston, Texas 77030 [D. W.]

ABSTRACT

Purpose: **Clinical studies have revealed that tumors may recur at the operative site if radioresistant *p53* mutation-positive residual disease remains in the body after treatment. Destruction of these remaining malignant cells, which can be present in both mucosal and deep muscle margins, may be achieved using *p53*-mediated gene transfer techniques. Most preclinical studies designed to assess the feasibility of harnessing this approach have used s.c. tumor models in nude mice, but it is anticipated that transduction of tumor cells in the muscle in immune-competent hosts may be more difficult.**

Experimental Design: **To address this point a new rodent model of residual cancer was established implanting PDVC57B tumor cells to create multiple tumor tracts in the muscle of syngeneic immune-competent C57Bl/6 mice. s.c. tumors and a s.c. model of residual disease were used as comparators.**

Results: **In the s.c. model of residual disease a single administration of 5×10^{10} viral particles of Ad5CMV-*p53* suppressed the growth of encapsulated tumor at the treatment site in six of six animals, but two of these animals had viable nests of tumor outside of the encapsulated zone. However, Ad5CMV-*p53* had no apparent effect on tumor cell progression in the model of residual cancer in the muscle. Creating the muscle model of residual cancer with a lower number of cells in the initial inoculum showed that immune-mediated effects, as well as those attributable to the transgene, are important in preventing tumor outgrowth. The frequency of transduction of tumor cells in the muscle, as determined after administration of Ad-β-*galactosidase*, was typically <3% and markedly different from the 20% transduction observed for the s.c. tumor model.**

Conclusions: **These studies highlight the need to devise strategies to improve delivery of adenovirus-mediated gene transfer to nests of tumor in muscle before this modality is used to treat residual cancer at this site. These may involve approaches such as intravascular delivery, strategies to improve vector diffusion, or combination with chemotherapy or radiotherapy to enhance gene delivery at these less accessible sites of disease.**

INTRODUCTION

Head and neck cancer represents a major health problem, as evidenced by its high incidence in many parts of the world, the poor survival rates, and the severe functional and cosmetic defects accompanying this disease and its treatment. Despite advances in all of the treatment modalities locoregional recurrence remains the most important cause of death for these patients. Recent studies, using a molecular diagnostic test based on finding the same *p53* gene mutation in a primary tumor and the surrounding normal tissue to detect occult tumor, reveal that this treatment failure is frequently because of the presence of residual cancer (1, 2). In our latest report, molecular evidence of residual cancer was found in both mucosal and deep muscle surgical margins (3). At present, the significance of finding a *p53* mutation in mucosal margins is unclear, but the presence of this aberration in muscle biopsies clearly identifies residual cancer, which may be responsible for the demise of the patient. Repeat surgery for these patients is not always feasible, and adjuvant radiotherapy is frequently used in an attempt to destroy any remaining malignant cells. The decision on whether or not to give postoperative radiotherapy is based on established clinicopathological criteria, and the result obtained with the molecular diagnostic is not taken into account. However, a proportion of cases with occult *p53* mutation-positive residual tumor develop a recurrence, even though they receive full-dose postoperative radiotherapy (3). Whether this treatment fails to prevent recurrence because these patients have tumors that are clinically aggressive, because they lack functional p53 or harbor other genetic abnormalities which modulate radiosensitivity, is not clear at present. Nevertheless, these investigations show that more of the same adjuvant treatment will not necessarily enable clinicians to cure more patients and highlight the requirement to devise new strategies to deal with residual cancer, which may be refractory to conventional approaches.

Head and neck tumors occur at reasonably accessible sites, such that these patients are good candidates for direct gene transfer to eliminate this residual disease. Recent advances in our understanding of the genetic basis of carcinogenesis have led to several strategies involving manipulation of the genetic information within tumor cells for therapeutic gain (reviewed in

Ref. 4). To date, most studies have focused on replacement of the *p53* tumor suppressor gene, because this sequence is mutated in ~60% of head and neck cancers (5).

Adenovirus-mediated gene transfer has been used for therapy of cancers arising in the head and neck because of its ability to infect both quiescent and dividing cells, to be grown to a high titer, and to produce transient expression of the target gene. Preliminary studies, introducing the *p53* gene into human tumor cells using an adenoviral vector, revealed inhibition of tumor growth and induction of apoptosis *in vitro* and in s.c. tumors *in vivo* (6, 7), and the results from the recently completed Phase I and II clinical trials, treating patients with locoregionally recurrent head and neck SCC,[2] also appear promising (8–10). At present, the exact mechanisms by which the *p53* gene product produces tumor-specific cell killing are unclear, although transfer of this sequence modulates expression of c-*myc* and *bax* (11), and neovascularization (12, 13).

In addition to significant clinical efficacy after direct intratumoral infection of localized tumor masses, Clayman *et al.* (14) have shown that adenovirus-mediated transfer of the *p53* gene prevents tumor outgrowth in a preclinical rodent model of *p53* mutation-positive minimal residual cancer in the s.c. tissue, mimicking the clinical scenario where malignant cells persist in mucosal surgical margins. However, residual cancer is frequently present in muscle biopsies (3), and transduction of tumor nests at this critical site, where diffusion is limited, may require a different approach. In this study we have used a rodent cell line forming tumors that are able to invade and grow in muscle and bone to create a preclinical model with multiple tracts of tumor in the muscle of a syngeneic, immune-competent host. Three isogenic vectors carrying a marker gene (Ad-β-*gal*), *p53* (Ad5CMV-*p53*), and a control "empty" vector (Ad-empty) were used to rigorously test the ability of *p53*-mediated gene transfer to destroy minimal residual tumor at this site. This model should also be useful in testing the benefits of *p53*-mediated gene transfer in various combination approaches, and when delivering novel treatments via different routes and testing alternative schedules of administration as a way to more aggressively treat minimal residual cancer at less accessible sites.

MATERIALS AND METHODS

Cell Lines and Culture Conditions. PDVC57B (15) and CarB (16) SCC lines were obtained from Cancer Research Campaign Technologies (London, United Kingdom). PDVC57B is syngeneic for C57Bl/6 mice and carries a *p53* mutation at codon 231, ATG-GTC (17), and an A-T transversion at codon 61 of the H-*ras* gene (15). HN5 is a SCC line harboring a *p53* mutation at codon 23 (18). Cells were maintained in DMEM supplemented with 10% fetal bovine serum and 1% penicillin/streptomycin.

---

[2] The abbreviations used are: SCC, squamous cell carcinoma; β-gal, β-galactosidase; CMV, cytomegalovirus; vp, virus particle; X-gal, 5-bromo-4-chloro-3-indolyl-β-D-galactopyranoside; TUNEL, terminal deoxynucleotidyl transferase (Tdt) -mediated nick end labeling; Ab, antibody.

Recombinant Adenovirus Preparation and Infection of Cells *in Vitro*. An E1-deleted replication-deficient recombinant adenovirus encoding wild-type *p53* cDNA under the control of the human CMV immediate early promoter (Ad5CMV-*p53* RPR/INGN201) was used to deliver the therapeutic target (6, 19). Vector lacking *p53* cDNA (Ad-empty) served as a control, and adenovirus carrying the Ad-β-*gal* gene was used to determine transduction efficiency (6, 17). Infection was carried out after washing cells with PBS by the addition of the virus to DMEM with 2% fetal bovine serum (Life Technologies, Inc., Paisley, Scotland) to cell monolayers. The cells were incubated at 37°C for 4 h; complete medium was added and incubation continued at 37°C. All of the experiments were performed in triplicate.

Cell Growth Assay and Cell Cycle Analysis. Cells were plated at a density of 2×10^5 in triplicate and infected with Ad5CMV-*p53*, Ad-β-*gal* or Ad-empty with 625-2500 vp/cell. For the growth assay, cells were harvested every day, counted, and their viability determined by trypan blue exclusion. For cell cycle analysis, 10^6 cells were infected with each of the three isogenic vectors. After 24 and 48 h trypsinized cells were mixed with those floating in the medium, washed, fixed, resuspended in RNase-A, and stained with 18 µg/ml propidium iodide. The percentage of cells in each phase of the cell cycle was determined by fluorescence-activated cell-sorting.

Transduction with β-Gal Adenovirus. PDVC57B cells (5×10^5) were incubated for 24 h at 37°C, with 650-5000 vp/cell Ad-β-*gal* for 4 h. Subsequently, 2 ml of complete medium was added, and incubation continued for 24 h at 37°C. Plates were washed twice in PBS, fixed with 3.7% formaldehyde in PBS for 10 min at 4°C, washed again, and stained with 1 mg/ml X-gal solution in 10% (w/v) *N,N*-dimethylformamide, 1.2 mM MgCl$_2$, 3.0 mM K$_4$FeCN, and 3.0 mM K$_3$FeCN, for 24 h at room temperature. Cells were counterstained with hematoxylin and the proportion of X-gal-positive cells assessed by light microscopy. At least 1000 cells were counted for each experiment and scored as positive if either diffuse or punctate blue staining was observed.

Detection of Expression from the *p53* Transgene. Total RNA was isolated from PDVC57B cells infected with 2500 vp/cell of each of the three isogenic vectors using RNA STAT-50 (Biogenesis, Poole, United Kingdom). The RNA was DNase-treated and reverse transcription performed at 22°C for 10 min and then at 42°C for 20 min using 1 µg RNA/reaction. The specific primers used for the promoter/*p53* region of Ad5CMV-*p53* were CMV2, 5′ GGTGCATTGGAACGCG-GATT 3′ and reverse exon 3, 5′ CAAATCATCCATTGCTT-GGGA 3′. A subsequent nested amplification was performed using CMV2 and an internal reverse primer, 5′ GGGGACA-GAACGTTG TTTTC 3′. The amplification reaction involved denaturation at 92°C for 1 min, and annealing at 58°C for 1 min and 72°C for 1 min for 35 cycles. Human glyceraldehyde-3-phosphate dehydrogenase primers were used as a positive control (5′ CAGCCG AGCCACATC-3′ and 5′-TGAGGCTGTT-GTCATACTTCT-3′). PCR products were resolved on 1% agarose gels and visualized by ethidium bromide staining. To ensure that we were not generating false-positive signals because of DNA contaminating RNA preparations, minus reverse transcriptase controls were included in all of the experiments.

Detection of cellular p53 was accomplished by Western blotting after infection with 2500 vp/cell Ad5CMV-*p53* or Ad-empty for 4–48 h. Cells were lysed in Laemmli sample buffer (62 mM Tris base, 10% w/v glycerol, 2% w/v SDS, 5% β mercaptoethanol, 1 μg/ml leupeptin, 1 μg/ml aprotinin, and 100 μg/ml phenylmethylsulfonyl fluoride). After centrifugation, 40 μg of protein was subjected to 10% SDS-PAGE and transferred to nitrocellulose. The membrane was blocked with 3% w/v BSA in Tris-buffered saline-Tween 20 (0.05% w/v Tween 20 in 1 × Tris-buffered saline) and probed with Ab248 (which is specific for mouse p53, diluted 1:500; a kind gift from D. Lane, Dundee University, United Kingdom), Ab DO1 (which reacts with human p53 but is only weakly cross-reactive with the mouse protein; Autogen Bioclear, Calne, United Kingdom; diluted 1:100), and actin (Sigma, Poole, United Kingdom; diluted 1:100) for 1 h. After incubation with an appropriate second layer the reaction was detected by chemiluminescence after the addition of 10 ml of 100 mM Tris-HCl (pH 8.5) mixed with 50 μl of 250 mM luminol in DMSO, 25 μl of 90 mM p-coumaric acid in DMSO, and 3 μl w/v H_2O_2 before autoradiography.

Immunohistochemical staining for p53 was performed with DO1 and 248 using the MOM immunodetection kit (Vector, Peterborough, United Kingdom) on cell monolayers infected with Ad5CMV-*p53* or Ad-empty, and 5-μm tissue sections, after fixation in 3.8% formalin and treated with 3% H_2O_2 in methanol for 5 min.

Apoptosis Detection: DNA Fragmentation Analysis. Cells (1×10^6) plated in triplicate were transduced with each of the three isogenic vectors at 2500 vp/cell. A similar number of cells were exposed to UV light for 2 min or to 20 μg/ml cisplatin. After various time intervals, adherent cells were lysed in DNA-STAT 60 (Biogenesis) and the supernatant centrifuged to collect the floating cells, which were disrupted in this lysate. Each sample (5 μg) was subjected to gel electrophoresis in a 1% agarose gel.

TUNEL Assay. Cells (1×10^6) plated in triplicate were transduced with each of the three isogenic vectors at 2500 vp/cell. After incubation for 24, 48, 60, and 72 h, floating cells were collected by centrifugation and resuspended in PBS on microscope slides coated with 5 μg/ml Cell-Tak tissue adhesive (Becton Dickinson, Oxford, United Kingdom) and air-dried before fixing in 4% paraformaldehyde for 30 min at room temperature. Adherent cells were fixed in a similar manner. After permeabilization for 2 min at 4°C in 0.1% Triton X-100 in 0.1% sodium citrate, TUNEL assay was performed using the *In Situ* Cell Death Detection kit, with fluorescein dUTP (Roche Diagnostics United Kingdom Ltd., Lewes, United Kingdom) according to the manufacturers' instructions.

Morphological Visualization of Apoptotic Cells. The medium containing the floating cells and the adherent cells after trypsin treatment were centrifuged and resuspended in PBS, and stained immediately with ethidium bromide and acridine orange (Sigma); 100 μg/ml of both stains were used (1:1 v/v) before fixation with 4% paraformaldehyde (20).

Establishment of s.c. Tumors and a s.c. Model of Minimal Residual Cancer. Female C57Bl/6 mice (7–8 weeks old) were obtained from Harlan Ltd. (Oxford, United Kingdom). The effect of Ad5CMV-*p53* on s.c. PDVC57B tumor nodules was determined in syngeneic mice. All of the experiments were approved by the Local Ethical Committee. To create s.c. tumor nodules after introduction of anesthesia with halothane, 5×10^6 cells in 50 μl of PBS were injected into the s.c. tissues over the right anterior and posterior flanks. Animals were observed daily, sacrificed on day 21, and tumors excised for histopathological examination. The s.c. model of minimal residual cancer was created as described by Clayman *et al.* (14). Briefly, female mice were anesthetized with halothane, and 5×10^5 PDVC57B cells were introduced in 50 μl of PBS into the s.c. tissue via two incisions, created in the right anterior and posterior flanks, which were sealed with sutures. After 48 h the mice were reanesthetized, the flap opened, and 5×10^{10} vp of Ad5CMV-*p53* or Ad-β-*gal* in 50 μl of PBS delivered to the posterior flank, using the needle to deposit the virus all around the s.c. pocket. The virus dispersed readily into the surrounding tissues, and the area was closed with sutures. Animals were observed daily and sacrificed on day 21. Tumors arising were removed and fixed in formalin for 12 h, embedded in paraffin wax, and 3-μm sections prepared and stained with H&E for microscopic examination.

Establishment of a New Model of Minimal Residual Cancer in the Muscle Bed. PDVC57B cells were implanted under halothane anesthesia into the lateral and medial heads of the gastrocnemius or rectus femoris muscle of female C57Bl/6 mice after exposure of the muscle via a skin incision. The tumor cells were introduced into the muscle in 40 μl of PBS using a gas-tight syringe (Hamilton, Carnforth, United Kingdom) and a short, 30-gauge needle with multiple parallel passes of the needle, typically injecting into the center of the muscle and into each of the four quadrants, without withdrawing the needle from the muscle after the first injection. The wound was closed with interrupted sutures. Mice were sacrificed on days 2–5, and the muscle exposed and removed for histological examination. To allow evaluation of the number and size of the tumor tracts forming at the midpoint and to establish how far they extended through the muscle, the central portion was excised and examined in cross-section, and the two remaining areas sectioned longitudinally before fixation in formalin for 24 h and embedding the specimen in paraffin wax. Alternatively, the entire muscle was embedded and histological sections prepared every 400-μm.

Inhibition of s.c. Tumor Growth *in Vivo*. To establish the efficacy of gene transfer in s.c. tumors developing in groups of six rodents, 5×10^{10} vp of Ad5CMV-*p53* or Ad-β-*gal* in 50 μl of PBS were injected into the nodules with multiple passes of the needle at different levels in one plane followed by a second series of passes in a plane at right angles to this. In some experiments, the virus was injected at random at different levels in multiple planes or a single injection was given. Biopsies were taken 24 and 48 h later for X-gal and p53 protein expression and after 5 days to evaluate the effect of treatment with Ad5CMV-*p53*. For β-*gal* reporter gene assay, tissues were snap-frozen in ornithine carbamyl transferase in isopentane over liquid nitrogen and stored at −80°C. Tissue sections (5-μm) were fixed in 3.7% formaldehyde for 10 min and stained with X-gal as described above. After 24 h, tissue sections were washed, counterstained in hematoxylin, and the percentage of positively stained blue cells determined by light microscopy.

Inhibition of Residual Cancer in the Muscle Bed. Rodents harboring multiple tracts of tumor in the muscle bed,
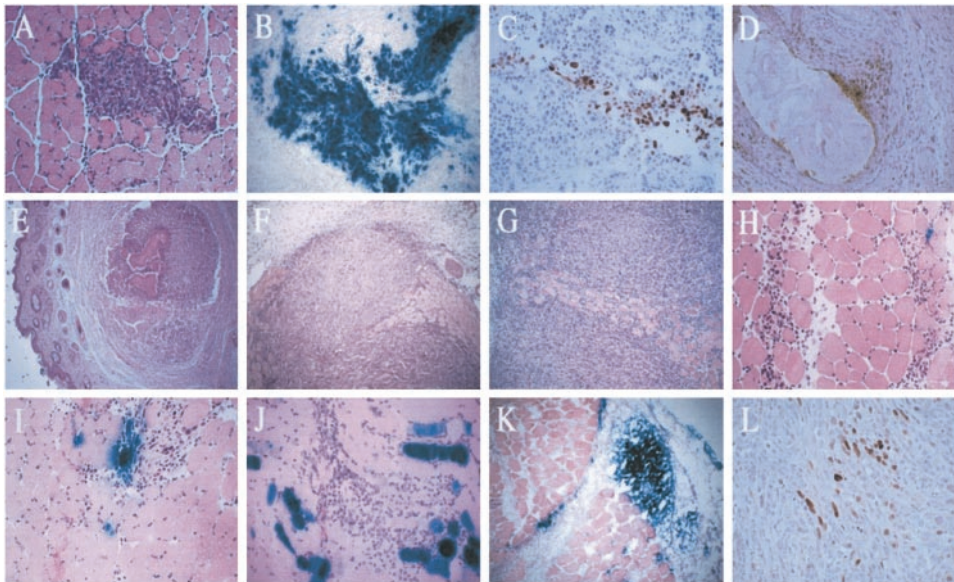
Fig. 1 Photomicrographs showing: *A*, model of minimal residual cancer in the muscle, tumor tract in the rectus femoris muscle; *B* and *C*, s.c. tumor, (*B*) X-gal staining and (*C*) p53-positive tumor; *D* and *E*, s.c. minimal residual cancer treated with Ad5CMV*p53*, (*D*) p53-positive tumor cells, and (*E*) dead and dying cells; *F–L*, minimal residual cancer in the muscle treated with (*F and G*) Ad5CMV*p53* or (*H–K*) Adβ*gal*, (*F*) coalescence of tumor tracts day 8, (*G*) expanding tumor mass day 10, (*H*) isolated X-gal positive cell, (*I*) positive myofibrils and cells at the periphery of a tumor tract, (*J*) X-gal positive myofibrils surrounding tumor focus, and (*L*) positive cells in loose connective tissue around the muscle. Magnification: *A,* ×230; *B,* ×140; *C,* ×285; *D,* ×260; *E, F,* and *K,* ×90; and *G,* ×115.

developed after implantation of 5×10^5 cells (as used to create the s.c. residual cancer model), were reanesthetized, the muscle exposed via a skin incision, and 5×10^{10} vp of Ad5CMV-*p53*, Ad-β-*gal*, or Ad-empty in 50 μl or PBS was delivered. Six mice were treated with each of the three isogenic vectors or PBS. The virus was injected into the muscle on days 4, 6, and 8 after implantation of the tumor cells with a series of passages of the needle in the long axis of the muscle followed by additional injections in a plane at right angles to this. In some experiments, virus was injected at random, at different levels in multiple planes, or with one or more passes of the needle through a single puncture in the fascia. The rodents were sacrificed 3 days after the final treatment with Ad5CMV-*p53*, Ad-empty, or PBS, and after 24 and 48 h after delivery of Ad-β-*gal*. Alternatively, 4 days after tumor cell implantation, groups of six mice were treated with i.p. cisplatin at 3 mg/kg on days 4, 6, and 8, and sacrificed on day 11.

Histopathological Examination. Biopsy specimens were evaluated for tumor content, apoptosis, necrosis, and the presence of inflammatory cell infiltrates after standard H&E staining. The number of tracts forming in the muscle was recorded at the various levels examined by light microscopy on coded slides by two observers (M. P. and R. O.) who were blinded to the treatment of the individual mice. The area of the tumor nests at each level was estimated as the product of the two greatest perpendicular dimensions at right angles, multiplied by π/4. Approximately one-third of tumor tracts had a circular shape, whereas the remainder had a more irregular appearance, with extension of tumor between the muscle fibers. When determining the area of these tumor tracts the perpendicular dimensions measured were those where tumor cells comprised at least 80% of the tissue examined, and irregular extensions of tumor into the surrounding muscle were considered to contribute to the overall mass only when at least five nuclei could be detected in each column of invading tumor cells. Columns comprising fewer malignant cells adjacent to the main tumor mass but having more than five nuclei at the periphery were not included when these measurements were taken. Any cystic spaces were counted as part of the tumor area. Inevitably this approach means that the area of tumors with a circular shape is estimated more precisely than that of tracts with markedly concave shapes, the size of which is overestimated using this approach. Photomicrographs and subsequently a Leica Q500 IW image workstation with QWin image processing and analysis software were used to measure the area of the tumor tracts at given points along the muscle.

Data Analysis. The number and cross-sectional area of tumor tracts developing at the midpoint of the gastrocnemius or rectus femoris muscles and the cross-sectional area of each tract were determined as described above. The total cross-sectional area of the tumor tracts developing in each muscle (calculated by summating the area of the individual tracts) and the average area (sum of the tumor tracts ÷ the number forming) were investigated as possible outcome measures. The midpoint was chosen to provide a simple and reproducible methodology, which is not influenced by *post-hoc* examination of the data. Estimates of the variation in cross-sectional area of the individual tumor tracts within and between mice were derived using ANOVA, and these results used to estimate variance when the areas of several tracts were averaged for each mouse. Interoperator reliability was assessed using the interclass correlation. To investigate the reliability of measuring total tumor area using

a single cross-section within a given muscle, the adjacent section on either side of the midpoint was rated and reliability obtained from ANOVA. This analysis could not be undertaken to assess the reliability of measuring average tumor tract area, as on some occasions the number of tumor tracts differed from one section to the next. This was perceived to be one advantage of using total tumor area rather than the average area of the tracts as an outcome measure. When all tracts of tumor fused the greatest perpendicular dimensions of the mass were measured as outlined above. Statistical comparisons of treatment groups, using either total tumor area or average tumor tract area as the outcome, were performed using parametric methods.

RESULTS

Development of a Model of Minimal Residual Cancer in the Muscle Bed. Preliminary experiments revealed that implantation of $1–5 \times 10^5$ PDVC57B cells into the gastrocnemius or rectus femoris muscle, with five passes of the needle, resulted in the formation of one to five tumor tracts after 2–4 days, mimicking the clinical scenario where residual cancer persists in the muscle after surgery. The average cross-section of the tracts developed with 10^5 cells and measured at the midpoint of the muscle after 4 days was 0.19 mm^2 (see Fig. 1A for representative example).

Implantation of 10^6 cells did not result in tumor tracts with a larger cross-sectional area, because the majority of these tracts formed internal cysts and did not grow well. In addition, when 10^6 cells were implanted, tumor cells were frequently identified growing between the lateral and medial heads of the gastrocnemius muscle and out into the surrounding connective tissue. Implantation of 10^4 cells typically resulted in formation of one to two tumor tracts, and although viable tumor cells were present, they often appeared dormant for 12–17 days before irregular outgrowths of cells appeared.

To establish the variability in the number of tumor tracts forming 4 days after implantation of PDVC57B cells with five passes of the needle, histological cross-sections of tumor-bearing muscles were prepared for eight mice. The number of tumor tracts developing at the midpoint ranged from three to five, and the maximum number, assessed by examination of cross-sections every 400 μm through the muscle, ranged from three to six (data not shown). Examination of semiserial cross-sections revealed that the tumor tracts did not always pass through the entire length of the muscle, although four or five tumor tracts were counted at >50% of levels examined for all of the rodents.

The appearance of fewer than five tumor tracts at the midpoint could have been because of fewer than five developing after implantation, two or more tracts coalescing, or to one or more tracts not passing through the midpoint of the muscle. However, where tracts have coalesced, the cross-sectional area of the combined tumor mass should be greater than that for a single tract. The relationship between the number and cross-sectional area of the individual tracts forming at the midpoint in the gastrocnemius and rectus femoris muscles is shown in Fig. 2. These data do not show that the area of a given tumor tract is related to the number observed, indicating that fusion of tracts is not a common event. This suggests that, as long as the number of tracts remains variable, average tumor tract area is a
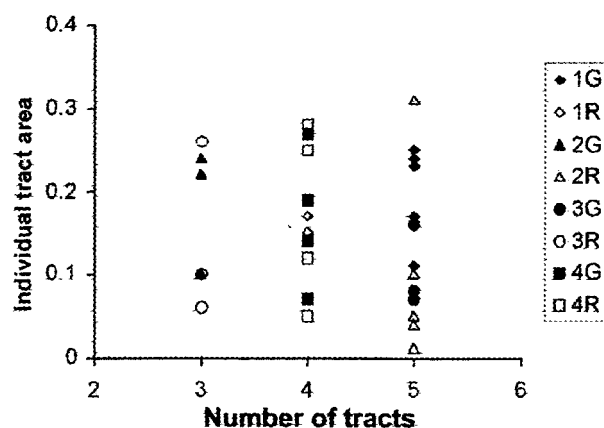

Fig. 2 Relationship between the number and area of individual tumor tracts developed in the gastronemicus (*G*) and rectus femoris (*R*) muscle. Eight representative examples are shown.

better outcome measure than total tumor area, because the latter increases when more tracts are present.

Although the cross-sectional areas of tumor tracts were constrained to be ≥0, Fig. 2 shows that their distribution is not noticeably skewed, allowing the results to be analyzed without applying a transformation. Using ANOVA, the variation in the area of individual tumor tracts in the gastrocnemius and rectus femoris muscles was partitioned into the variation between mice (gastrocnemius SD, 0.040 mm^2; rectus femoris SD, 0 mm^2) and within mice (gastrocnemius SD, 0.063 mm^2; rectus femoris SD, 0.101 mm^2). From these figures the SD of an average of the areas of several tumor tracts in the same muscle was estimated. The average of five tumor tracts was predicted to have an SD of 0.049 mm^2 in the gastrocnemius muscle and 0.045 mm^2 in the rectus femoris, with the corresponding figures for the average of three tumor tracts being 0.054 mm^2 and 0.058 mm^2. In comparison, the SD of the area of a single tract was 0.075 mm^2 for the gastrocnemius and 0.101 mm^2 for the rectus femoris. Averaging the area of the tumor tracts reduced the variability more in the rectus femoris muscle, because there was estimated to be less variation in the tracts developing at this site between mice than when the gastrocnemius was used. Although the SD depends on the number of tracts being averaged, which will vary in practice as found in the present study, this provides useful information for planning studies to test the efficacy of a novel therapeutic agent. Given the variability of the outcome, the statistical power of any study will depend on the sample size and the effect of the chosen treatment. Table 1 shows how large the effect of treatment (that is, the mean difference in the average cross-sectional area between the test and control groups) needs to be in order for the study to have 80% power at the 5% significance level, for representative sample sizes. For example, when tumor tracts are created in the rectus femoris, aiming to produce five tracts in each muscle, a study of 24 mice (12 test and 12 control) will have 80% power at the 5% significance level to detect a mean difference between the two groups of 0.06 mm^2. In general, these values are insensitive to the number of tumor tracts being averaged, so the variability in the latter does not prevent use of these figures as a guide when testing the

Table 1 Assessment of the size of the treatment effect,[a] which can be demonstrated with 80% power at the 5% significance level using different sample sizes, where the outcome measure is the average cross-sectional area of three or five tumor tracts or total tumor area

Sample size	Gastrocnemius			Rectus femoris		
	No. of tracts			No. of tracts		
	3	5	Total area	3	5	Total area
6	0.09	0.08	0.38	0.10	0.08	0.20
12	0.07	0.06	0.27	0.07	0.06	0.14
24	0.05	0.04	0.19	0.05	0.04	0.10
48	0.04	0.03	0.14	0.04	0.03	0.07

[a] Mean difference in mm^2 between treated and control groups.

efficacy of novel treatments if some muscles contain fewer tumor tracts than anticipated because of the inherent biological variation associated with this model system.

The total cross-sectional tumor area measured at the midpoint ranged from 0.47 to 1.00 mm^2 in the gastrocnemius muscle (mean, 0.68 mm^2; SD, 0.23 mm^2) and from 0.42 to 0.70 mm^2 in the rectus femoris (mean, 0.54 mm^2; SD, 0.12 mm^2; data not shown). As with average tumor tract area, the estimates of variability in the total tumor area can be used where this is the primary outcome of the preclinical studies (see Table 1). For example, using the above SDs as estimates of the population SDs, we find that in order for a study comparing a treated with a control group to have 80% power at the 5% significance level, the mean difference in tumor area in the gastrocnemius muscle needs to be 0.19 mm^2 for a study with 24 mice/group and 0.38 mm^2 with 6 mice/group. The mean difference in tumor area in the rectus femoris is also shown.

To assess the interoperator reliability, the same histological sections were independently assessed by another operator. As anticipated, there was perfect agreement on the number of tracts recorded at the midpoint for each case. A total of 33 tracts were measured by both operators: 17 in gastrocnemius muscles and 16 in rectus femoris. The intraclass correlation for the area of an individual tract was 0.74 mm^2 in the gastrocnemius muscle and 0.95 mm^2 for the rectus femoris. When total tumor area was calculated from the results of each operator, the intraclass correlation was 0.92 for the gastrocnemius and 0.96 for the rectus femoris. The within-muscle reliability of total tumor area measured from a single section was 0.64 for the gastrocnemius and 0.62 for the rectus femoris. Averaging the areas measured from three adjacent sections increased this reliability to 0.84 for the gastrocnemius and 0.83 for the rectus femoris.

Adenovirus Infection of PDVC57B Cells: Transduction Efficiency with Ad-β-*Gal*. Transduction efficiency of PDVC57B cells was assessed after infection with Ad-β-*gal* by counting the number of blue cells after X-gal staining. Cells inoculated with a single dose of 2500 vp/cell of Ad-β-*gal* consistently expressed almost 100% blue cells, whereas 650 and 1250 vp showed 60–80% positive cells (data not shown).

Effect of Exogenous *p53* on PDVC57B Cell Growth *in Vitro*. Cells infected with Ad-empty or Ad-β-*gal* had growth rates similar to those of the mock-infected cells, whereas growth of cells infected with Ad5CMV-*p53* was significantly suppressed (Fig. 3). Forty-eight h after infection with Ad5CMV-*p53*, morphological changes appeared in a proportion of the cell
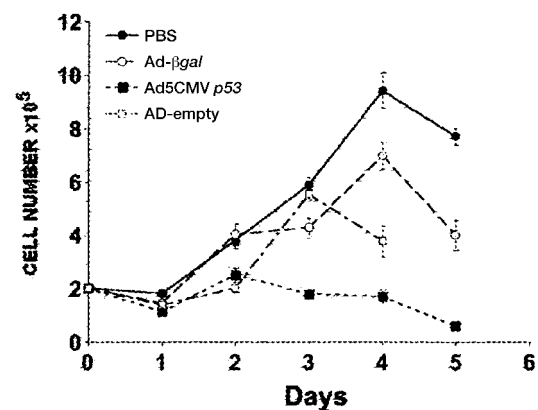

Fig. 3 Inhibition of PDVC57B tumor cell growth *in vitro*. The mean of the cell counts in triplicate wells after infection is plotted against the number of days since infection; *bars,* ± SE.

population, such that apoptotic cells with condensed and fragmented nuclei could be distinguished from normal cells. Cells infected with Ad-empty or Ad-β-*gal* showed normal growth characteristics with no abnormal morphological appearance. Ad5CMV-*p53* at 625 vp/cell reduced PDVC57B cell numbers by >50% after 72 h. These findings indicate that the vectors is efficient at eliminating these cells and that the transduction efficacy of Ad5CMV-*p53* in PDVC57B cells is higher than reported for Tu-138, used to establish the s.c. model of minimal residual disease in an earlier report (14). However, the *in vitro* and *in vivo* experiments reported in the present investigation were carried out with 2500 vp/cell (equivalent to 100 plaque-forming units) and 5×10^{10} vp, respectively, to ensure high viral titer.

Expression of Exogenous p53 in Adenovirus-infected PDVC57B Cells. After infection of PDVC57B cells with 2500 vp/cell for 2–24 h total RNA was isolated. *p53* transcripts were detected after 4 h in PDVC57B and CarB cells transduced with Ad5CMV-*p53*, whereas this was not present in reverse transcription-negative controls, the parental, Ad-β-*gal*, or Ad-empty-infected cells (Fig. 4A). Immunocytochemistry with AbDO1 revealed that infection of PDVC57B cells with Ad5CMV-*p53* resulted in expression of human p53 in the cytoplasm after 18 h and in the nucleus after 24–48 h. Expression of the transgene was detected at 6 h and maintained for at least

Fig. 4 A, detection of transgene expression after adenoviral-mediated *p53* gene transfer. Uninfected PDVC57B cells (*Lane 1*), PDVC57B cells infected with 2500 vp/cell Ad-empty (*Lane 2*) or Ad5CMV-*p53* (*Lanes 3* and *4*) and CarB infected with Ad5CMV-*p53* (*Lane 5*) were subjected to reverse transcription-PCR analysis using CMV promoter/p53 exon 3 or glyceraldehyde-3-phosphate dehydrogenase primers; *B*, Western blot analysis, cellular extracts from PDVC57B cells 48 h after infection with 2500 vp/cell Ad-empty (*Lane 1*), Ad5CMV-*p53* (*Lane 2*), and uninfected HN5 cells (*Lane 3*). Murine p53 is detected with Ab 248; human p53 with Ab DO1.

Table 2 Effect of infection with Ad5CMV-*p53* and Ad-empty on the percentage of PDVC57B cells in each phase of the cell cycle as determined by fluorescence-activated cell sorting

Cell cycle	Ad5CMV-*p53*	Ad-empty	PBS
G_1%	10	36	60
S%	12	17	12
G_2-M%	28	44	25
Sub-G_1%	50	3	3

60 h. Western blotting revealed a *p53* band recognized by AbDO1 in cellular extracts isolated from PDVC57B cells infected with Ad5CMV-*p53* (Fig. 4*B*) and HN5 but not from untreated cells or those infected with Ad-empty. (Levels of human *p53* were higher than the endogenously mutated mouse *p53*, indicating that the exogenous *p53* mRNA is efficiently translated into immunoreactive p53 protein.

Detection of Apoptosis. Twenty-four h after infection of adherent PDVC57B cells with Ad5CMV-*p53*, few apoptotic cells (~2%) were detected in the adherent population whereas >95% of the floaters were TUNEL-positive, and the number of TUNEL-positive apoptotic floating cells increased proportionally to the duration of Ad5CMV-*p53* infection, with >5000 cells detected after 72 h. In contrast, only a modest increase in the number of apoptotic floaters was detected at this time after infection of cells with Ad-β-gal or Ad-empty. These data correlate well with the effect of Ad5CMV-*p53* on the growth rate of PDVC57B cells. Apoptosis was also demonstrated by morphological assessment and acridine orange/ethidium bromide uptake, as the medium containing the floating cells, after infection of adherent cells for 72 h with Ad5CMV-*p53*, contained cells with red fluorescent nuclei and nuclear fragmentation (late apoptotic cells), and a proportion of adherent cells (typically <5%) showed green fluorescence and condensed nuclei after 48 h (early apoptotic cells; data not shown). Apoptosis was confirmed by the finding of an increase in the population of hypodiploid sub-G_1 (apoptotic cells) after treatment with Ad5CMV-*p53* (50%) *versus* Ad-empty (3%; Table 2). The appearance of DNA fragments, equivalent to ~200 bp and their multiples, was noted in PDVC57B cells after treatment with cisplatin after 48 h, but no detectable DNA fragments were visualized after infection with Ad5CMV-*p53* or Ad-empty (data not shown).

Infection of s.c. Tumor Nodules with Ad5CMV-*p53* and Ad-β-*Gal*. After injection of 5×10^5 PDVC57B cells into the flanks of syngeneic hosts, s.c. tumor nodules were apparent after 21 days. Macroscopically, the tumor sizes ranged from 7 to 10 mm in diameter. Histologically, the s.c. tumors were spindle-cell carcinomas with areas of squamous differentiation. They were typically encapsulated by fibrous tissue but invaded into the surrounding muscle after 21–30 days. The majority of tumors developed areas of central necrosis at this time.

Subcutaneous tumors created in immune-competent hosts were infected with each of the three isogenic vectors. After infection with Ad-β-*gal*, ~20% of the tumor cells were positively stained with X-gal (Fig. 1*B*). In some cases, areas of tumor along needle tracts were stained, whereas in other cases only scattered blue cells were observed. The number of blue cells was greater when multiple injections were given in different directions rather than using a series of passes in one plane followed by a second series of injections in a plane at right angles to this. Seventy-two h after infection with Ad5CMV-*p53*, areas of the tumor were found to express p53 protein by immunohistochemistry (Fig. 1*C*), and sheets of dead and dying cells were detected by morphological assessment and TUNEL assay after 48–60 h.

Seventy-two h after molecular therapy with 5×10^{10} vp of Ad5CMV-*p53* to suppress growth of minimal residual cancer in the s.c. tissue, p53 protein was detected by immunohistology (Fig. 1*D*). Tumor nodules developed in zero of six anterior flanks after 3 weeks. Histological examination of these sites revealed a mass of dead cells, liquefaction, and chronic inflammation, surrounded by a connective tissue capsule (Fig. 1*E*). However, viable nests of tumor were found outside of the encapsulated zone in two mice treated with Ad5CMV-*p53* at this time. In contrast, all of the mice treated with Ad-empty developed tumors in the posterior flanks.

Model of Minimal Residual Cancer in the Muscle Bed. Treatment of muscles harboring a maximum of five tumor tracts, 4 days after implanting 5×10^5 PDVC57B cells, with three doses of 5×10^{10} vp of Ad5CMV-*p53* or Ad-empty did not reduce the number or the area of the tumor tracts measured at the midpoint of the muscle. A few days after treatment commenced there was an initial increase in the number of neutrophils and monocytes, and after 7 days many cytotoxic T lymphocytes appeared (data not shown). Two days after the final treatment with Ad5CMV-*p53*, histological assessment of sections prepared at the midpoint of the tumor-bearing muscles revealed coalescing tumor tracts (Fig. 1*F*), which progressed to form a single tumor mass, in six of six mice treated with this vector (Fig. 1*G*). The mean cross-sectional area of the fused tracts was broadly similar for the animals treated with Ad5CMV-*p53*, Ad-β-*gal*, and empty vector (Ad5CMV-*p53* range, 2.17–5.78 mm^2 and mean, 4.07 ± 0.73; Ad-β-gal range, 2.25–5.53 mm^2 and mean, 3.81 ± 0.64; and Ad-empty range, 2.52–4.95 mm^2 and mean, 3.45 ± 0.49). This finding was confirmed by preparation of serial sections every 400 μm through the muscle. Comparison of the tumor area after treat-

Table 3 The effect of treatment with cisplatin (A) and PBS (B) on the number and area of the tumor tracts developing in the gastrocnemius muscle

A. Cisplatin

Mice	No. of tracts	Cross-sectional area					Total area
		1	2	3	4	5	
1	1	0.29				0.29	
2	5	0.25	0.18	0.37	0.24	0.31	1.35
3	3	0.22	0.12	0.12			0.46
4	4	0.27	0.18	0.38	0.28		1.11
5	1	0.47					0.47
6	2	0.18	0.16				0.34

B. PBS

Mice	No. of tracts	Cross-sectional area					Total area
		1	2	3	4	5	
1	4	0.31	0.72	0.47	0.20		1.70
2	5	1.15	0.62	0.47	0.16	0.42	2.82
3	5	0.49	0.29	0.39	0.52	0.31	2.00
4	5	0.48	0.22	0.38	0.25	1.00	2.33
5	4	0.86	0.47	0.39	0.64	0.01	2.37
6	5	0.39	0.59	0.48	0.33	0.47	2.26

ment with Ad5CMV-*p53* and Ad-empty showed no significant difference between the two groups ($t = 0.90$; degrees of freedom, 10; $P = 0.391$).

X-gal staining of frozen sections of tumor-bearing muscles biopsied 48 h after injection of Ad-β-*gal*, delivering the virus with multiple passes of the needle into different areas of the muscle through a single puncture in the fascia, revealed that <3% of the tumor cells expressed this transgene (for examples see Fig. 1, *I* and *J*). Occasional positive myofibres and inflammatory cells were also seen. More X-gal-positive myofibres were seen when a quilting technique was used to deliver the virus (Fig. 1*J*), but staining of cells in the loose connective tissue around the muscle blocks was also increased (Fig. 1*K*), suggesting leakage of the vector out of the muscle through the multiple perforations in the facsia. Rare foci of p53-positive tumor cells were detected by immunohistochemistry in the tumor-bearing muscles 48 h after the final treatment with Ad5CMV-*p53* (Fig. 1*L*) when the tumor burden was significant. Because the transduction efficiency was not improved by varying the injection protocol this shows that improving retention of vector within tumor-bearing muscles will be pivotal if adenovirus-mediated gene transfer is to be used to target small foci of residual tumor at this site.

When these experiments were repeated with rodents harboring tumor tracts developed after implantation of 10^5 PDVC57B cells and three doses of 5×10^{10}vp of Ad5CMV-*p53* or Ad-empty were delivered, commencing treatment 2 days after tumor cell implantation, no difference was observed in the extent of tumor growth or the pattern of infiltration into the muscle when the effects of the two isogenic viruses were compared. However, when compared with rodents treated with PBS, which had developed a mass of tumor in the muscle because of coalescence of the individual tumor tracts, those treated with Ad5CMV-*p53* or Ad-empty developed a complex, spidery network of tumor cells, infiltrating between the muscle fascicles,

rather than forming discrete tumor tracts. In addition, many neutrophils and cytotoxic T lymphocytes were present within this network, as well as shrunken, dying cells. However, a single tract of dead and dying malignant cells, developing in the connective tissue outside of the muscle mass, was observed in a rodent treated with Ad5CMV-*p53*, showing that this treatment can destroy tumor tracts growing outside of the dense muscle tissue.

Treatment of rodents harboring tumor tracts in the muscle bed with 3 mg/kg cisplatin i.p. over 6 days reduced the number of tumor tracts forming (range 1–5 in the cisplatin treated group, $n = 6$; range 4–5 in the PBS control group, $n = 6$; Table 3). When compared with PBS-treated controls, the tumor tracts developing in rodents treated with cisplatin contained more ghost cells and showed less invasion into the surrounding tissue, although some spidery outgrowths were still present. Because the number of tumor tracts which had developed in each rodent after tumor cell implantation was not known, the average tumor tract area after treatment with cisplatin could not be calculated, and total tumor area was used as the outcome measure. Rodents treated with this cytotoxic were found to have a significantly lower total tumor area than the group treated with PBS ($t = 5.97$; degrees of freedom, 10; $P = 0.0001$; cisplatin mean, 0.67 mm^2; range, 0.29–1.35 mm^2; $n = 6$; PBS mean, 2.25 mm^2; range, 1.70–2.83 mm^2; $n = 6$).

DISCUSSION

Gene therapy relies heavily on experimentation in animal models to establish proof of principle before therapeutic efficacy can be established in clinical trials. Rodent models with cancer and minimal residual cancer in the s.c. flanks of immune-compromised rodents provide an idea of the value of novel approaches *in vivo* (7, 14). However, clinical studies have revealed that occult residual tumor is frequently present in both

muscle and mucosal surgical margins (3), and transducing tumor cells within the muscle, where diffusion is limited, may not be straightforward.

The development of a novel rodent model with multiple tracts of tumor capable of invading into the muscle of a syngeneic, immune-competent host is an important step forward and will facilitate preclinical studies to devise effective strategies to destroy tumor cells, which remain in deeper structures. Our experiments show that it is possible to create a model of minimal residual cancer in the muscle bed by implanting $1–5 \times 10^5$ PDVC57B cells with five parallel passes of the needle through the gastrocnemius or rectus femoris muscle of C57Bl/6 mice. Using this technique, after 4 days three to five tumor tracts are formed of average area 0.19 mm^2 at the midpoint, mimicking the clinical scenario where small nests of tumor may be present at multiple sites within the muscle. In the present study, fewer tumor tracts comprising cells, which tended to remain dormant, were observed when 10^4 cells were implanted, and injection of 10^6 cells produced areas of tumor, which frequently contained cystic cavities, strongly suggesting that the number and size of the tracts created must be established empirically for each new cell line tested. Examination of semiserial sections revealed that an equal number of tumor tracts did not necessarily develop at every level examined. This may reflect heterogeneity in the tumor cell population. Alternatively, tumor cells may be squeezed along the tissue planes if the muscle contracts when the needle is withdrawn. Nevertheless, development of multiple tracts of tumor provides an opportunity to rigorously test the efficacy of gene transfer or other novel therapeutic approaches to destroy residual tumor in the muscle.

As anticipated, our findings show that different therapeutic agents have different effects on tumor growth and highlight the need to devise a series of strategies to measure these at a given point, selected as the midpoint of the muscle in the present study. Examination of adjacent sections allowed us to calculate the variability in the size of the tumor tracts, between and within mice, and determine the numbers of rodents that should be included in test and control groups to detect a significant treatment effect with a new drug (Table 1). The present model has been developed with a squamous cell tumor line harboring a *p53* gene mutation, which allows the efficacy of protocols to restore the function of this sequence to be tested. The use of syngeneic immune-competent rodents also allows the contribution of immune-mediated effects to be assessed, because the lack of an immune response to a vector may spuriously enhance the extent and duration of any gene-mediated therapeutic effect. It is well recognized that adenoviral vectors elicit both a humoral and a cellular immune response in syngeneic hosts (21), and the high number of polymorphonuclear cells and cytotoxic T lymphocytes detected in the tumors treated with Ad5CMV-*p53* and Ad-empty, but not in tumors mock-infected with PBS, suggests that inflammation may participate in the efficacy of these agents *in vivo* (22). This model can also be created by introducing human tumor cells into the muscle of immune-compromised rodents to create tracts of tumor at this site, providing that the cell line selected has characteristics that permit growth in this tissue.

In vitro studies transducing PDVC57B cells with β-*gal* showed that nearly 100% of tumor cells were positive after X-gal staining, establishing the presence of adenovirus receptors. In addition, infection of these cells with Ad5CMV-*p53* resulted in significant growth reduction *in vitro*, as compared with mock-infected cells or those infected with Ad-empty, showing that the mechanism by which wild-type *p53* inhibits tumor growth *in vitro* is virus-mediated and not a nonspecific effect. After infection of PDVC57B cells with Ad5CMV-*p53*, apoptosis was detected by morphological assessment, TUNEL, and cell cycle analysis. However, DNA fragmentation was not observed after transduction of PDVC57B cells with Ad5CMV-*p53*, although treatment with cisplatin produced characteristic DNA laddering. Similar findings have been reported for other tumor cells lines. For example, the growth of H358 (a human non-small cell lung cancer cell line, in which both alleles of *p53* are deleted) is inhibited by Ad5CMV-*p53*, but DNA fragmentation does not occur (19), and these different responses are likely to reflect the various genetic backgrounds of the tumor lines tested.

Ad5CMV-*p53* was effective in destroying PDVC57B cells forming s.c. nodules in syngeneic immune-competent mice *in vivo*. However, X-gal staining after infection with Ad-β-*gal* shows that, whereas the efficiency of transduction in s.c. tumor models in nude mice is acknowledged to be variable and typically 30–60% (23), only 10–20% of malignant cells express this transgene when similar tumors are created in immune-competent hosts. In addition, four of six rodents harboring minimal residual cancer in the s.c. tissue, treated with Ad5CMV-*p53*, did not show any histological evidence of viable malignant cells. However, in these experiments, nests of tumor were detected outside of the encapsulated mass of dead and dying cells in two rodents, suggesting that the ability of vector to reach or be retained at these sites may have been reduced relative to the encapsulated tumor mass.

Our experiments also suggest that the mechanisms by which cell death occurs after *p53* gene transfer may differ in immune-competent and nude mice. Forty-eight h after transduction of s.c. tumor nodules with Ad5CMV-*p53*, sheets of TUNEL-positive dead and dying cells were observed, surrounded by an inflammatory cell infiltrate consisting of neutrophils and monocytes. It is well recognized that distinguishing between apoptosis and necrosis is not always straightforward. The TUNEL method labels apoptosis and necrotic cells, and, characteristically, apoptosis affects scattered individual cells and is not associated with inflammation, whereas necrosis usually involves contiguous cells. Thus, the finding of sheets of TUNEL-positive cells in the present study suggests that tumor cell death, after infection of immune-competent hosts with Ad5CMV-*p53*, occurs as a result of both processes. Necrosis may also be precipitated by tissue hypoxia because of the *p53* transgene affecting angiogenesis (12, 13).

Injection of Ad5CMV-*p53* into muscle harboring multiple tumor tracts did not prevent tumor outgrowth, and the tracts coalesced to produce a mass with a similar area to that developing after treatment with Ad-empty. In contrast to the negative results observed after delivery of Ad5CMV-*p53*, treatment of rodents implanted with similar numbers of tumor cells with i.p. cisplatin reduced both the number and area of the tumor tracts. Examination of histological sections taken from tumor-bearing muscles stained with X-gal, 2 days after transduction with

Ad-β-*gal*, strongly suggests that the percentage of tumor cells expressing the transgene in the muscle is very low (<3%) when compared with the levels of transduction (typically 20%) observed after injection of Ad5CMV-*p53* into s.c. tumor nodules. In the present study, the vector was delivered into the tumor-bearing muscles with injections that were typically <2 mm apart. The paucity of X-gal expression reveals that diffusion and convection of adenoviral vectors through tumor-bearing muscles is significantly reduced when compared with s.c. tumors, such that only scant transduction of residual tumor in muscle occurs. These findings indicate that direct injection of adenoviral vectors directly into the muscle bed after tumor resection, with the aim of eliminating any residual cancer, is unlikely to be successful even though the tumor-bearing area is widely exposed at that time.

Treatment of tumor tracts, developing 2 days after implantation of fewer (10^5) PDVC57B tumor cells with Ad5CMV-*p53* or Ad-empty, had an equal effect in terms of limiting tumor cell proliferation and reduced the tumor burden when compared with PBS-treated rodents. The inhibitory effect of empty vectors, because of retention of immunogenic sequences in the backbone, is known to be greatest when the tumor burden is small and levels of the vector are high (22), a finding which is confirmed in the present study. These empty vectors may inhibit tumor growth by transduction of tumor or endothelial cells, by influencing other growth regulatory factors and immune-mediated events in the tumor milieu. Evidence from the present study, showing heavy infiltration of tumor-bearing muscles, treated with Ad-empty, by neutrophils and cytotoxic T lymphocytes, strongly supports the notion that immune-mediated effects, which are independent of the transgene, are important in preventing outgrowth of low numbers of tumor cells. In addition, PDVC57B rodent tumors are heavily infiltrated with monocytes, and exposure of monocytes to adenovirus results in release of tumor necrosis factor and IFNs, which may also play a role in tumor suppression in the present model (reviewed in Ref. 24). Thus, whereas tumor cell killing attributable to p53-mediated induction of apoptosis, necrosis, and effects on angiogenesis probably all contribute to tumor cell destruction when efficient transduction of tumor cells is achieved, the results seen in adenoviral-treated animals over those observed in PBS-treated controls indicate that immune-mediated effects are also important.

The present investigation highlights the need to improve delivery of adenovirus-mediated gene transfer to tumor in muscle or to use combination therapies without overlapping toxicities to increase selective and specific tumor cell killing. To date, no dose-limiting toxicity has been observed in clinical trials using Ad5CMV-*p53* (8, 25, 26), suggesting that systemic or regional treatment may be tolerable. Intravascular therapy has the potential to improve delivery to the tumor site, and when combined with strategies to maximize diffusion of vector around the muscle fascicles, may address the challenges posed by the need to deliver vectors to tissues where diffusion is limited. Because systemic treatment also has the potential to prevent development of distant metastases, additional preclinical studies to assess the feasibility of these approaches are warranted.

REFERENCES

1. Brennan, J. A., Mao, L., Hruban, R. H., Boyle, J. O., Eby, Y. J., Koch, W. M., Goodman, S. N., and Sidransky, D. Molecular assessment of histopathological staging in squamous-cell carcinoma of the head and neck. N. Engl. J. Med., *332:* 429–435, 1995.

2. Partridge, M. Head and neck cancer and precancer: can we use molecular genetics to make better predictions? Ann. R. Coll. Surg. Engl., *81:* 1–11, 1999.

3. Partridge, M., Li, S-R., Pateromichelakis, S., Francis, R. A., Phillips, E., Huang, X-H., Tesfa-Selase, F., and Langdon, J. D. Detection of minimal residual cancer to investigate why oral tumors recur despite seemingly adequate treatment. Clin. Cancer Res., *6:* 2718–2725, 2000.

4. Partridge, M. Current status of genetics for prediction, prognosis and gene therapy. Acta Oto-Laryngologica, *8:* 69–80, 2000.

5. Partridge, M., Kiguwa, S., Emilion, G., Pateromichelakis, S., A'Hern, R., and Langdon, J. D. New insights into p53 protein stabilization in oral squamous cell carcinoma. Eur. J. Cancer B Oral Oncol., *35:* 45–55, 1999.

6. Liu, T-J., Zhang, W-W., Taylor, D. L., Roth, J. A., Goepfert, H., and Clayman, G. L. Growth suppression of human head and neck cancer cells by the introduction of a wild-type *p53* gene via a recombinant adenovirus. Cancer Res., *54:* 3662–3667, 1994.

7. Liu, T-J., El-Naggar, A. K., McDonnell, T. J., Steck, K. D., Wang, M., Taylor, D. L., and Clayman, G. L. Apoptosis induction mediated by wild-type *p53* adenoviral gene transfer in squamous cell carcinoma of the head and neck. Cancer Res., *55:* 3117–3122, 1995.

8. Clayman, G., El-Naggar, A. K., Lippman, S. M., Henderson, Y. C., Frederick, M., Merritt, J. A., Zumstein, L. A., Timmons, T. M., Liu, T. J., Ginsberg, L., Roth, J. A., Hong, W. K., Bruso, P., and Goepfert, H. Adenovirus-mediated *p53* gene transfer in patients with advanced recurrent head and neck squamous cell carcinoma. J. Clin. Oncol., *16:* 2221–2232, 1998.

9. Clayman, G. L., Frank, D. K., Bruso, P. A., and Goepfert, H. Adenovirus-mediated wild-type *p53* gene transfer as a surgical adjuvant in advanced head and neck cancers. Clin. Cancer Res., *5:* 1715–1722, 1999.

10. Goodwin, W. J., Esser, D., Clayman, G. L., Neumanitis, J., Yver, A., and Dreiling, L. J. Randomized Phase II study of intratumoral injection of two dosing schedules using a replication-deficient adenovirus carrying the *p53* gene (Ad5CMV-p53). J. Clin. Oncol., *18:* 1717A, 1999.

11. Frederick, M. J., Holton, P. R., Hudson, M., Wang, M., and Clayman, G. L. Expression of apoptosis-related genes in human head and neck squamous cell carcinomas undergoing *p53*-mediated programmed cell death. Clin. Cancer Res., *5:* 361–369, 1999.

12. Dameron, K. M., Volpert, O. V., Tainsky, M. A., and Bouck, N. Control of angiogenesis in fibroblasts by p53 regulation of thrombospondin-1. Science (Wash. DC), *265:* 1582–1584, 1998.

13. Nishizaki, M., Fujiwara, T., Tanida, T., Hizuta, A., Nishimori, H., Tokino, T., Nakamura, Y., Bouvet, M., Roth, J. A., and Tanaka, N. Recombinant adenovirus expressing wild-type *p53* is antiangiogenic: a proposed mechanism for bystander effect. Clin. Cancer Res., *5:* 1015–1023, 1999.

14. Clayman, G. L., El-Naggar, A. K., Roth, J. A., Zhang, W-W., Goepfert, H., Taylor, D. L., and Liu, T-J. *In vivo* molecular therapy with *p53* adenovirus for microscopic residual head and neck squamous carcinoma. Cancer Res., *55:* 1–6, 1995.

15. Quintanilla, M., Haddow, S., Jonas, D., Jaffe, D., Bowden, G. T., and Balmain, A. Comparison of ras activation during epidermal carcinogenesis *in vitro* and *in vivo*. Carcinogenesis (Lond.), *12:* 1875–1881, 1991.

16. Diaz-Guerra, M., Haddow, S., Bauluz, C., Jorcano, J. L., Cano, A., Balmain, A., and Quintanilla, M. Expression of simple epithelial cytokeratins in mouse epidermal keratinocytes harboring Harvey ras gene alterations. Cancer Res., *52:* 680–687, 1992.

17. Burns, P. A., Kemp, C. J., Gannon, J. V., Lane, D. P., Bremner, R., and Balmain, A. Loss of heterozygosity and mutational alterations of the

p53 gene in skin tumors of interspecific hybrid mice. Oncogene, *6:* 2363–2369, 1991.

18. Easty, D. M., Easty, G. C., Carter, R. L., Monaghan, P., and Butler, L. J. Ten human carcinoma cell lines derived from squamous carcinomas of the head and neck. Br. J. Cancer, *43:* 772–785, 1981.

19. Fujiwara, T., Grimm, E. A., Mukhopadhyay, T., Zhang, W-W., Owen-Schaub, L. B., and Roth, J. A. Induction of chemosensitivity in human lung cancer cells *in vivo* by adenovirus-mediated transfer of the wild-type *p53* gene. Cancer Res., *54:* 2287–2291, 1994.

20. McGahon, A. J., Martin, S. J., Bissonnette, R. P., Mahboubi, A., Shi, Y., Mogil, R. J., Nishioka, W. K., and Green, D. R. The end of the (cell) line: methods for the study of apoptosis *in vitro*. Methods Cell Biol., *46:* 153–185, 1995.

21. Chirmule, N., Propert, K. J., Magosin, S. A., Qian, R., and Wilson, J. M. Immune responses to adenovirus and adeno-associated virus in humans. Gene Ther., *6:* 1574–1583, 1999.

22. Zhang, W-W., Alemany, R., Wang, J-X., Koch, P. E., Ordonez, N. G., and Roth, J. A. Safety evaluation of Ad5CMV-*p53 in vitro* and *in vivo*. Hum. Gene Ther., *6:* 155–164, 1995.

23. Cusack, J. C., Spitz, F. R., Nguyen, D., Zhang, W. W., Cristiano, R. J., and Roth, J. A. High levels of gene transduction in human lung tumors following intralesional injection of recombinant adenovirus. Cancer Gene Ther., *3:* 245–249, 1996.

24. Gooding, L. R., and Wold, W. S. M. Molecular mechanisms by which adenoviruses counteract antiviral immune defenses. Crit. Rev. Immunol., *10:* 53–71, 1990.

25. Swisher, S. G., Roth, J. A., Nemunaitis, J., Lawrence, D. D., Kemp, B. L., Carrasco, C. H., Connors, D. G., El-Naggar, A. K., Fossella, F., Glisson, B. S., Hong, W. K., Khuri, F. R., Kurie, J. M., Lee, J. J., Lee, J. S., Mack, M., Merritt, J. A., Nguyen, D. M., Nesbitt, J. C., Perez-Soler, R., Pisters, K. M. W., Putnam, J. B., Jr., Richli, W. R., Savin, M., Schrump, D. S., Shin, D. M., Shulkin, A., Walsh, G. L., Wait, J., Weill, D., and Waugh, M. K. A. Adenovirus-mediated *p53* gene transfer in advanced non-small-cell lung cancer. J. Natl. Cancer Inst., *91:* 763–771, 1999.

26. Nemunaitis, J., Swisher, S. G., Timmons, T., Connors, D., Mack, M., Doerksen, L., Weill, D., Wait, J., Lawrence, D. D., Kemp, B. L., Fossella, F., Glisson, B. S., Hong, W. K., Khuri, F. R., Kurie, J. M., Lee, J. J., Lee, J. S., Nguyen, D. M., Nesbitt, J. C., Perez-Soler, R., Pisters, K. M. W., Putnam, J. B., Richli, W. R., Shin, D. M., Walsh, G. L., Merritt, J., and Roth, J. Adenovirus-mediated *p53* gene transfer in sequence with Cisplatin to tumors of patients with non-small-cell lung cancer. J. Clin. Oncol., *18:* 609–622, 2000.

Clinical Cancer Research

A Preclinical Model of Minimal Residual Cancer in the Muscle Highlights Challenges Associated with Adenovirus-mediated *p53* Gene Transfer

Roth Oakley, Elaine Phillips, Richard Hooper, et al.

Updated version	Access the most recent version of this article at: http://clincancerres.aacrjournals.org/content/8/6/1984

Cited articles	This article cites 26 articles, 11 of which you can access for free at: http://clincancerres.aacrjournals.org/content/8/6/1984.full#ref-list-1
Citing articles	This article has been cited by 1 HighWire-hosted articles. Access the articles at: http://clincancerres.aacrjournals.org/content/8/6/1984.full#related-urls

E-mail alerts	Sign up to receive free email-alerts related to this article or journal.
Reprints and Subscriptions	To order reprints of this article or to subscribe to the journal, contact the AACR Publications Department at pubs@aacr.org.
Permissions	To request permission to re-use all or part of this article, use this link http://clincancerres.aacrjournals.org/content/8/6/1984. Click on "Request Permissions" which will take you to the Copyright Clearance Center's (CCC) Rightslink site.